NOAA Technical Memorandum NOS NGS 24

DETERMINATION OF THE GEOPOTENTIAL FROM SATELLITE-TO-SATELLITE TRACKING DATA

Rockville, Md
January 1980

noaa NATIONAL OCEANIC AND ATMOSPHERIC ADMINISTRATION / National Ocean Survey

NOAA Technical Publications

National Ocean Survey/National Geodetic Survey subseries

The National Geodetic Survey (NGS) of the National Ocean Survey (NOS), NOAA, establishes and maintains the basic National horizontal and vertical networks of geodetic control and provides governmentwide leadership in the improvement of geodetic surveying methods and instrumentation, coordinates operations to assure network development, and provides specifications and criteria for survey operations by Federal, State, and other agencies.

NGS engages in research and development for the improvement of knowledge of the figure of the Earth and its gravity field, and has the responsibility to procure geodetic data from all sources, process these data, and make them generally available to users through a central data base.

NOAA Technical Memorandums and some special NOAA publications are sold by the National Technical Information Service (NTIS) in paper copy and microfiche. Orders should be directed to NTIS, 5285 Port Royal Road, Springfield, VA 22161 (telephone: 703-557-4650). NTIS customer charge accounts are invited; some commercial charge accounts are accepted. When ordering, give the NTIS accession number (which begins with PB) shown in parentheses in the following citations.

Paper copies of NOAA Technical Reports, which are of general interest to the public, are sold by the Superintendent of Documents, U.S. Government Printing Office (GPO), Washington, DC 20402 (telephone: 202-783-3238). For prompt service, please furnish the GPO stock number with your order. If a citation does not carry this number, then the publication is not sold by GPO. All NOAA Technical Reports may be purchased from NTIS in hard copy and microform. Prices for the same publication may vary between the two Government sales agents. Although both are nonprofit, GPO relies on some Federal support whereas NTIS is self-sustained.

An excellent reference source for Government publications is the National Depository Library program, a network of about 1,300 designated libraries. Requests for borrowing Depository Library material may be made through your local library. A free listing of libraries currently in this system is available from the Library Division, U.S. Government Printing Office, 5236 Eisenhower Ave., Alexandria, VA 22304 (telephone: 703-557-9013).

NOAA geodetic publications

Classification, Standards of Accuracy, and General Specifications of Geodetic Control Surveys. Federal Geodetic Control Committee, John O. Phillips (Chairman), Department of Commerce, NOAA, NOS, 1974 reprinted annually, 12 pp (PB265442). National specifications and tables show the closures required and tolerances permitted for first-, second-, and third-order geodetic control surveys. (A single free copy can be obtained, upon request, from the National Geodetic Survey, C13x4, NOS/NOAA, Rockville MD 20852.)

Specifications To Support Classification, Standards of Accuracy, and General Specifications of Geodetic Control Surveys. Federal Geodetic Control Committee, John O. Phillips (Chairman), Department of Commerce, NOAA, NOS, 1975, reprinted annually, 30 pp (PB261037). This publication provides the rationale behind the original publication, "Classification, Standards of Accuracy, ..." cited above. (A single free copy can be otained, upon request, from the National Geodetic Survey, C13x4, NOS/NOAA, Rockville MD 20852.)

Proceedings of the Second International Symposium on Problems Related to the Redefinition of North American Geodetic Networks. Sponsored by U.S. Department of Commerce; Department of Energy, Mines and Resources (Canada); and Danish Geodetic Institute; Arlington, Va., 1978, 658 pp. (GPO #003-017-0426-1). Fifty-four papers present the progress of the new adjustment of the North American Datum at midpoint, including reports by participating nations, software descriptions, and theoretical considerations.

NOAA Technical Memorandums, NOS/NGS subseries

NOS NGS-1 Use of climatological and meteorological data in the planning and execution of National Geodetic Survey field operations. Robert J. Leffler, December 1975, 30 pp (PB249677). Availability, pertinence, uses, and procedures for using climatological and meteorological data are discussed as applicable to NGS field operations.

NOS NGS-2 Final report on responses to geodetic data questionnaire. John F. Spencer, Jr., March 1976, 39 pp (PB254641). Responses (20%) to a geodetic data questionnaire, mailed to 36,000 U.S. land surveyors, are analyzed for projecting future geodetic data needs.

(Continued at end of publication)

NOAA Technical Memorandum NOS NGS 24

DETERMINATION OF THE GEOPOTENTIAL FROM SATELLITE-TO-SATELLITE TRACKING DATA

B. C. Douglas, C. C. Goad and
F. F. Morrison

National Geodetic Survey
Rockville, Md.
January 1980

UNITED STATES
DEPARTMENT OF COMMERCE
Juanita M. Kreps, Secretary

NATIONAL OCEANIC AND
ATMOSPHERIC ADMINISTRATION
Richard A. Frank, Administrator

National Ocean
Survey
Herbert R. Lippold. Jr., Director

CONTENTS

DETERMINATION OF THE GEOPOTENTIAL FROM SATELLITE-TO-SATELLITE TRACKING DATA

Bruce C. Douglas
Clyde C. Goad
F. Foster Morrison

National Geodetic Survey
National Ocean Survey, NOAA
Rockville, Md. 20852

ABSTRACT. Simulations were made of the recovery of mean gravity anomalies from intersatellite Doppler measurements. A pair of surface-force compensated satellites was assumed to be in identical polar orbits, spaced by 3°, at an altitude of 200 km, taking intersatellite data with a precision of 0.001 mm/s. The results for a half-year mission indicate that 1°x1° mean gravity anomalies can be obtained to a precision of a few milligals. A so-called high-low case, when one of the satellites is geosynchronous, appears to perform about twice as well, but is probably impractical to use because of the difficulty in obtaining the required data precision (10^{-3} mm/s) with the long (~36,000 km) intersatellite distance involved. In contrast to previous analyses, our results are indicative of data obtainable from a global solution free of debatable a priori constraints or assumptions about the geopotential. Thus a properly optimized mission using additional information, such as results from altimetry or mean surface anomalies, could improve upon the results presented here.

INTRODUCTION

The concept of using intersatellite measurements to determine the geopotential is at least 10 years old (Wolff 1969). The advantage of this scheme, compared to those based on ground-based observations, is continuous global observation of orbital perturbations produced by the anomalous geopotential.

The long wavelength variations of the geopotential, e.g., $n \leq 6$, have been determined satisfactorily from conventional satellite tracking data. Progress also has been made at very short wavelengths using GEOS-3 altimeter data. Rapp (1979) reported 1°x1° mean gravity anomalies from these data precise to ~7 mgal over most of the ocean surface. However, a global determination of the gravity field to a higher precision would seem to depend on a new satellite system.

For a believable simulation of the recovery of gravity field parameters, the following conditions are necessary:

- The simulation should have a global character.
- The simulation should consider the effect of random and systematic errors.
- The simulation should be independent of a priori information.

The last requirement may appear stringent, but adherence produces conservative conclusions.

REPRESENTATION OF THE EARTH'S GRAVITY FIELD

Spherical harmonics were unsuitable for our analyses because a complete set of coefficients would have been required to model purely local effects. A spherical harmonic model of degree and order 180 (1°x1° resolution) would require 32,400 coefficients. In addition, the computation of harmonics above degree and order 70 requires special care (Chovitz et al. 1973). We chose instead to represent 1°x1° mean gravity anomalies by a surface layer of variable density. In particular, we assumed the density χ to be constant over a small block, and represented the total field in terms of an aggregation of such blocks.

Another representation, spherical harmonic sampling functions, has been proposed by Giacaglia and Lundquist (1972). However, these have severe computational problems. Sampling functions for a line, plane, or any

Cartesian Space R, can be generated by translation; i.e., one needs only to shift the argument by one division. For example, if we define

$$S_o(x) = \frac{\sin\ (2\pi x)}{2\pi x}$$

we can derive the remainder of the sampling functions from

$$S_k\ (x) = S_o\ (x - k), \quad k\ \ \pm 1, \pm 2, \ldots .$$

Unfortunately, a simple symmetry condition does not exist for the spherical domain, so one would have to invert 32,400 nonsparse matrices of dimension 32,400 x 32,400 to obtain the functions, which would be represented by a series with 32,400 terms. Thus, technical and economic considerations determined the use of a surface density model in these simulations. In addition, the ORAN (orbit analysis) computer program, described later, did not have to be modified and retested extensively before using the density model subroutines. The logic in Morrison's (1977) program was changed to accept blocks of arbitrary size (Morrison 1979). We did not use more sophisticated means of analyzing the results, such as inversion theory (Kaula et al. 1978) or collocation (Moritz 1978) because the project was designed to determine the sensitivity and resolution unique to the proposed satellite-to-satellite tracking systems.

The density of a block is related to the usual mean gravity anomaly Δg (Orlin 1959)

$$G\chi = \frac{\Delta g}{2\pi} + \frac{3}{2}\frac{\gamma}{R} N = \frac{\Delta g}{2\pi} + 0.0368\ N$$

where G is the gravitational constant, γ is global mean gravity, R is mean Earth radius, N is geoid height (m), χ is surface density, and Δg and $G\chi$ are in milligals. For most of the Earth, the approximation

$$\Delta g \approx 2\pi\ G\ \chi$$

suffices for the purpose of error analysis.

Computing the acceleration of a satellite resulting from a 1°x1° density layer block involves evaluation of a double integral. Some authors approximate the solution of this integral by the attraction of one or more point masses (Koch and Witte 1971). We used the solution of Morrison (1976, 1977). He evaluates one integral approximately analytically and the other integral numerically. The advantage of this latter scheme is that the block has no artificial "structure." Unless a very large number of point masses is used to approximate an individual density block, this structure creates rapidly oscillating perturbations on a low altitude orbit, possibly leading to erroneous conclusions.

The global rms (root mean square) mean gravity anomaly in 1° squares is about 30 mgal. Because the uncertainty of 1°x1° mean anomalies visible to GEOS-3 over the ocean surface is less than 10 mgal, let us consider the effect of a 10-mgal, 1°x1° block on the speed of a near-Earth satellite. Figure 1 shows the velocity perturbation in the along-track direction for a satellite in a circular polar orbit passing directly over the block at an altitude of 200 km.

Several interesting features appear in figure 1. First, note that the block has two effects, a small high frequency perturbation of about 0.006 cm/s, and a much larger low frequency (once/revolution) effect. This latter effect comes from the overall perturbation of the energy, and hence period (Hotine and Morrison 1969). The effect does not contribute information because every block will contain the effect and adjacent blocks cannot be separable on this basis since the wavelength of the effect is vastly greater than the dimensions of the blocks. The significant information about a block appears in the sharp high frequency oscillation which occurs as the satellite passes over a block. This oscillation persists, however, for a considerable time (2-3 minutes) compared to the time required for a satellite to traverse the 1°x1° block (0.25 minute). The fact that the perturbation of a block persists over an along-track distance of about 10 times the block size also means that adjacent 1°x1° blocks will have a similar effect. These will be hard to separate even when using the high frequency impulse. It is also apparent that to maximize the relative along-track velocity perturbation between two satellites in identical low orbits the separation of the satellites must be greater than 1°.

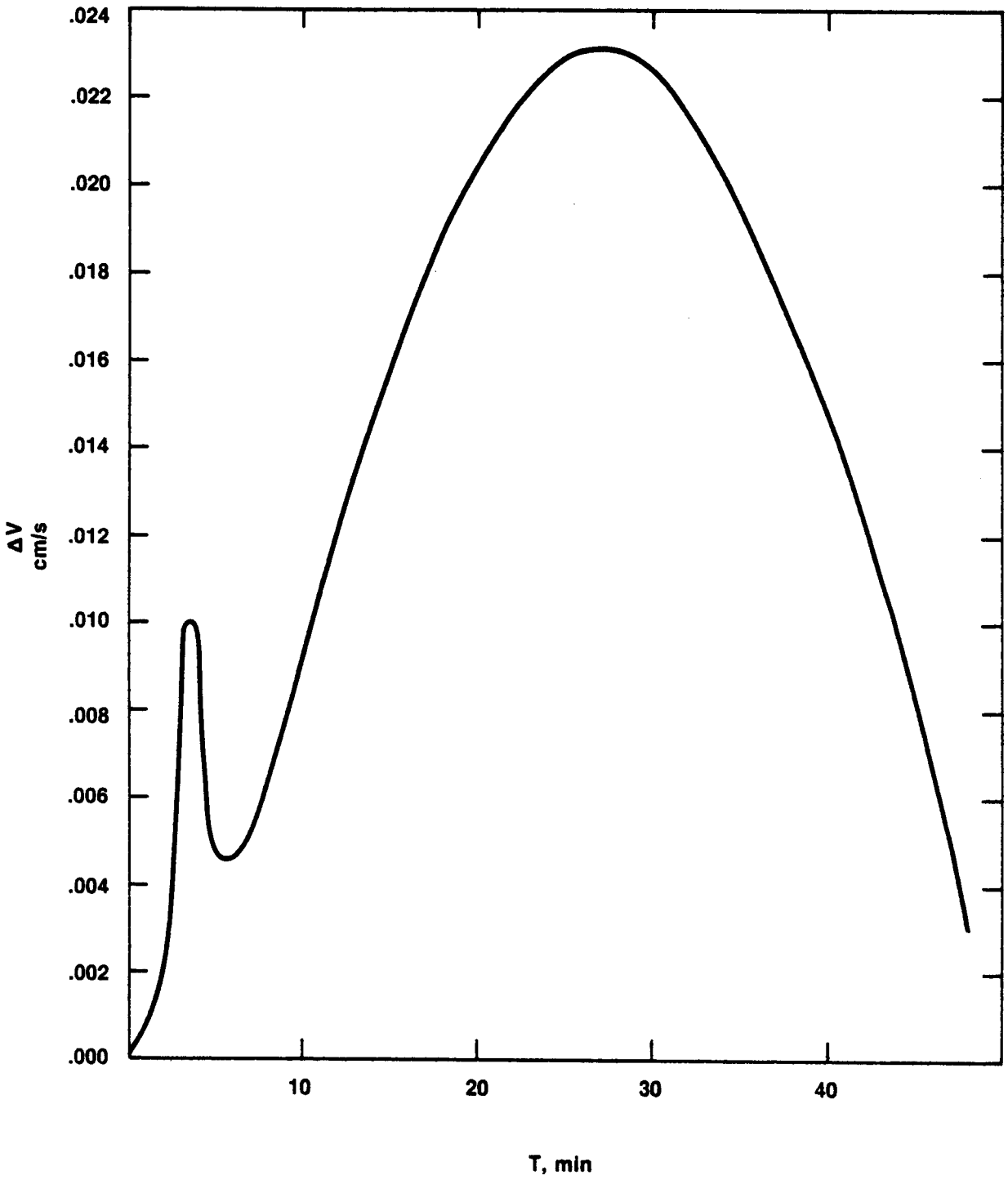

Figure 1.--The perturbation in the along-track component of velocity resulting from a 10-mgal, 1°x1° mean anomaly for a satellite at 200-km altitude.

The magnitude of the velocity perturbation could be increased by choosing a lower altitude, but 200 km is a reasonable height for a practical mission after considering atmospheric drag forces. At this altitude the atmospheric density scale height is only about 35 km, so the drag force is very sensitive to small changes in altitude. In the discussion that follows, we assume all satellites used surface-force compensation devices to eliminate drag and radiation pressure effects.

Figure 2 shows the relative speed (i.e., range-rate) between two satellites passing over the 10-mgal, 1°x1° anomaly (used in fig. 1) for various separations of the satellites. Larger separations yield a larger signal. Figure 3 shows the maximum signal occurs for a separation exceeding 5°. It is important to remember that the maximum signal is dependent on the altitude as well as the separation, causing figure 3 to be valid only for a 200-km altitude.

Figures 2 and 3 illustrate the essential problem of determining the fine structure of the gravity field from satellite perturbations. The effect of a 1°x1° block is very small. Thus, attempting to estimate the geopotential in terms of 1°x1° anomalies requires highly accurate data and attention to the effect of systematic errors.

SIMULATION METHOD

The most difficult aspect in simulating the recovery of the global geopotential from satellite-to-satellite tracking is the need for a global analysis. In our situation, we are interested in a resolution of 1°x1°, but there are 41,000 1°x1° equal-area blocks on the sphere. Solutions proposed by other authors have not been entirely satisfactory. Argientero et al. (1978) simulated the adjustment of a small region of 1°x1° blocks and carried the additional surrounding blocks as unadjusted parameters with a given variance in the solution. Schwarz (1971) also computed the covariance matrix of adjusted blocks in a limited region, but with the tacit assumption that the blocks which were not adjusted were known without error. Clearly the former approach leads to pessimistic results, the latter to optimistic conclusions.

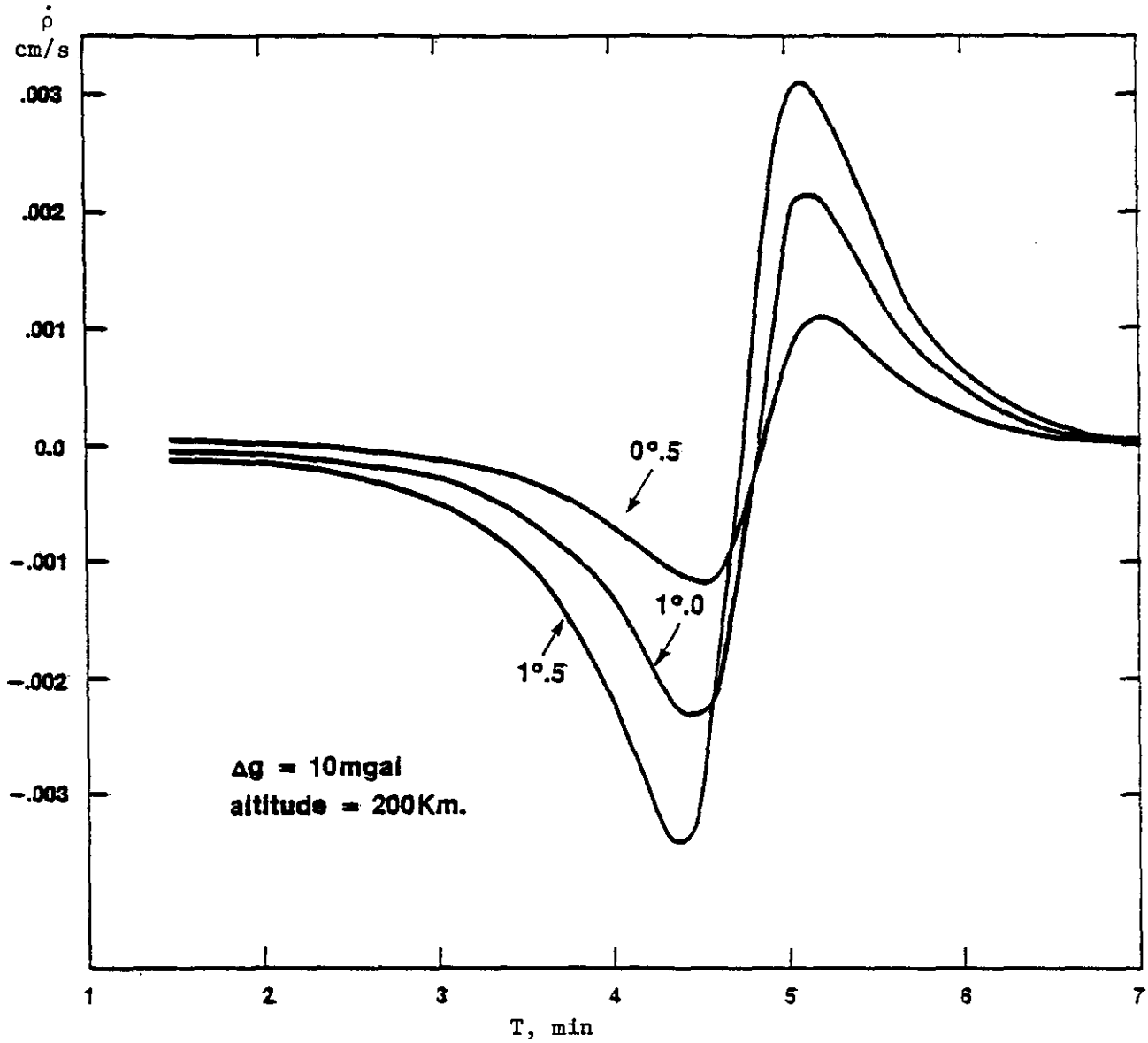

Figure 2.--Intersatellite relative speed ($\dot{\rho}$) for various separations of the satellites.

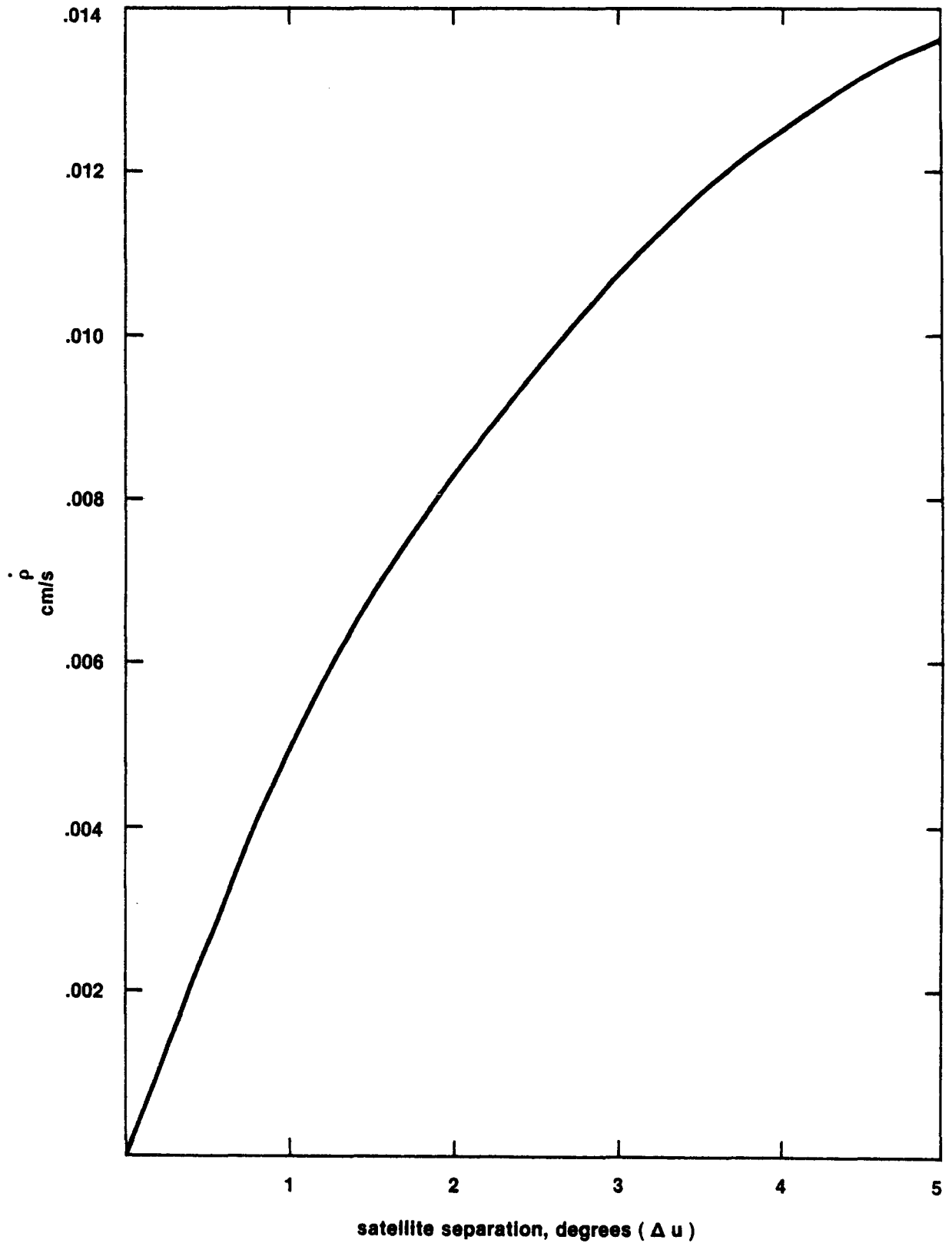

Figure 3.--Maximum variation of intersatellite range-rate ($\dot{\rho}$) for various satellite separations (Δu).

Our approach for simulating a global solution was to simulate the recovery of a region with dimensions large enough to allow the 1°x1° anomalies near the center of the region to be regarded as having essentially the same statistical properties in the solution that they would have possessed in a global solution. Figure 1 shows the size of this region would have to be substantial because the impulse-like perturbation of a 1°x1° block persists for a long time relative to the size of the block. We began our experiments with a 15°x15° region containing 225 1°x1° mean gravity anomalies. To verify that this region was large enough to ensure the central anomaly would have the properties of a global solution, we simulated the recovery of a larger 15°x25° region. Our results actually improved slightly for the central region, giving us confidence that our conclusions would be conservative.

Another problem in simulating the recovery of 1°x1° gravity anomalies is the tremendous amount of required orbital computations. In our example using a region 15° wide, many months of orbiting by polar satellites would have been required to obtain dense overflights of the area. In addition, a 5-second numerical integration step size, with a multistep method is required because of the sharp, high frequency effect of 1°x1° anomalies. To avoid this lengthy computation we considered independent orbital arcs only over the region being considered. However, the initial conditions for each arc were not adjusted. Our assumption was that the ephemerides of the two satellites would be computed in long arc (a few days) solutions from ground tracking.

The separation of the ephemeris computation from gravity anomaly estimation requires justification, especially in relation to the effect of systematic errors on the ephemerides. For example, the locations of ground tracking stations are uncertain to some degree, and this error propagates into the intersatellite range-rate measurement. Fortunately, this effect is readily evaluated.

The usual least-squares solution relates observation residuals, δO, to adjusted parameters, a, in the presence of data noise, e, by

$$\delta 0 = A\ \delta a + e \tag{1}$$

where A is a matrix of partial derivatives of the measurements with respect to the adjusted parameters. If unadjusted parameters with error, γ, related to the observations by a matrix of partials, K, are present, then the observation equation becomes

$$\delta 0 = A\ \delta a - K\ \gamma + e. \tag{2}$$

If W^{-1} is the covariance matrix of the measurement noise, e, the minimum variance solution $\delta\hat{a}$, which ignores the error in the unadjusted parameters, is biased by an amount

$$-(A^T\ W\ A)^{-1}\ A^T\ W\ K\ \gamma. \tag{3}$$

The effect of a unit value of the γ parameters is given by

$$\partial(\delta\hat{a})/\partial\gamma = -(A^T\ W\ A)^{-1}\ A^T\ W\ K. \tag{4}$$

By using eq. (4), for example, we can predict in advance the effects of an error in station location on any particular solution. This is important to evaluate, especially in the present case, because of the smallness of the perturbation of a 1°x1° mean gravity anomaly.

Although eq. (4) is simple in principle, it is computationally complex. For example, we can easily imagine a mission where 10 Doppler or laser ground tracking stations would each observe two satellites for 6 months. The partial derivative matrices A and K must be obtained by numerical integration of variational equations, and there are scores of these equations.

Many sources of potential systematic error can arise in orbit determination. The most prominent are geopotential and tracking station coordinate errors. We did not consider geopotential error here because we have assumed, of course, that the geopotential was being estimated. However, tracking-station coordinate errors need to be considered.

Using the computer program ORAN, which was developed around eq. (4), we determined the effect of a 10-cm uncertainty in the height of one station based on the initial conditions and the intersatellite range-rate measurement, $\dot{\rho}$, for two satellites spaced 3° apart in the same 200-km altitude polar orbit. The orbital arc length was 1 day with 15 Doppler tracking sites well-distributed around the globe, using line-of-sight velocity measurements of σ = 1 cm/s quality. The 10-cm value for the error of station coordinates is realistic for the 1985 time frame. Figure 4 shows the results.

Two significant aspects are apparent in figure 4. First, notice the long period of the oscillation produced by the station coordinate error. This effect, as noted before, occurs for orbital arcs more than a few revolutions long and is caused by the dynamics of orbital motion. With modern instruments, the timing error of observations is negligible, so that the orbital period is extremely well-determined in long-arc solutions by repeated passages over the tracking stations. Thus the satellite ephemeris can be in error only periodically, as seen in figure 4. The effect of an error in the location of an observing station is different from the effect of a localized gravity anomaly, such as a 1°x1° block, because the gravity anomaly causes a distinct local change in the acceleration of the satellite.

The other important feature of figure 4 is the smallness of the effect of the station coordinate error on the intersatellite range-rate. The amplitude is 2.5 x 10^{-4} cm/s, about 5 percent of the impulse-like effect of a 10-mgal, 1°x1° anomaly block. Because the wavelength of the station-error induced signal is more than 10 times the wavelength of the anomaly block effect, one would anticipate little aliasing of one signal into the other. But it is a simple matter to filter the intersatellite range-rate signal and eliminate the error signal. To illustrate this, the low amplitude curve in figure 4 shows the effect of the station height error on the intersatellite range-rate difference, $\Delta\dot{\rho}$ taken over 1 minute. Figure 5 shows the corresponding differences of the range-rate oscillation produced by the 10-mgal, 1°x1° block. As expected, the long wavelength signal is greatly reduced, and the high frequency impulse-like signal is amplified. In terms of

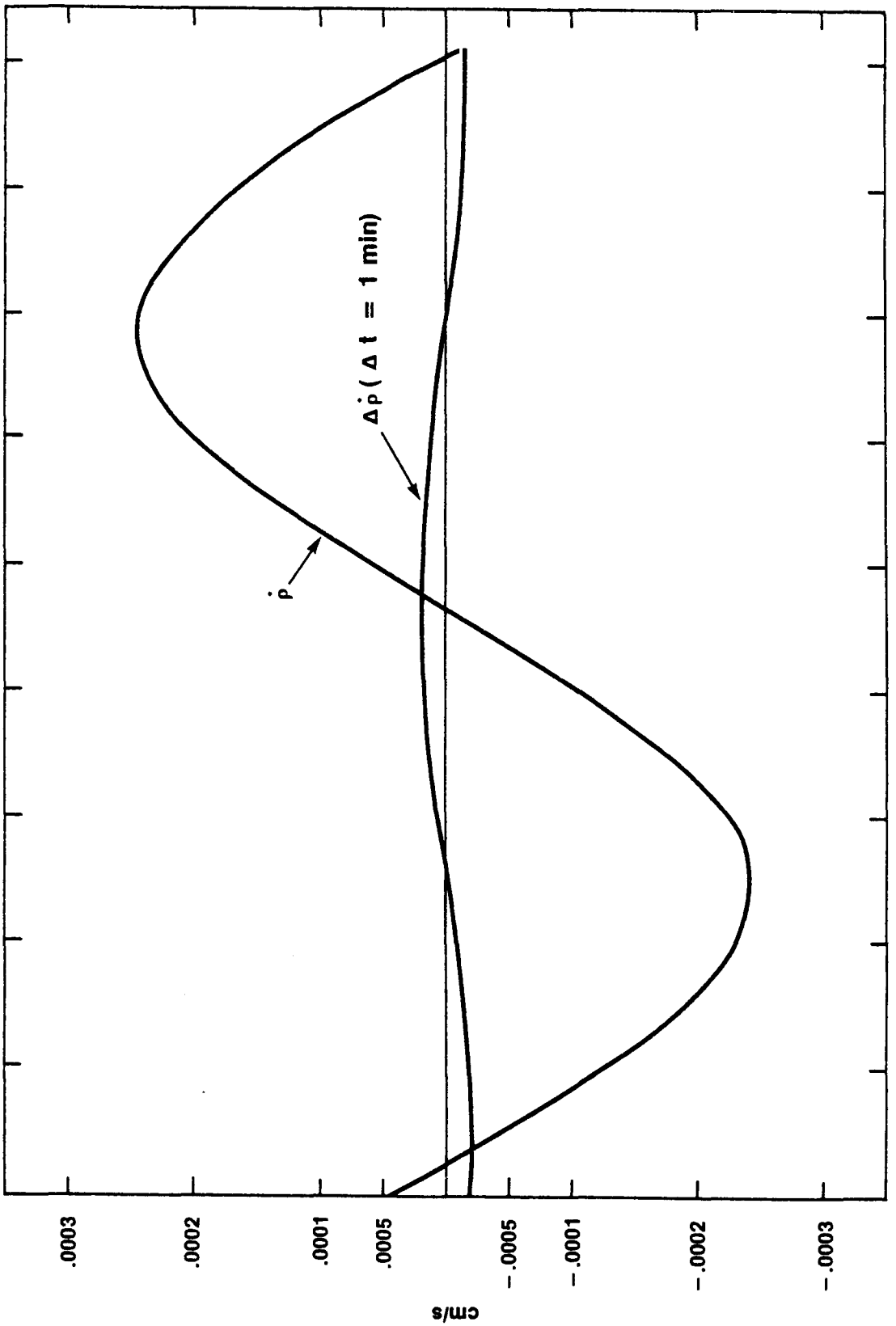

Figure 4.--The effect of a 10-cm station height error on the intersatellite range-rate and range-rate differences ($\Delta\rho_{max}$ = -2 x 10^{-5} cm/s).

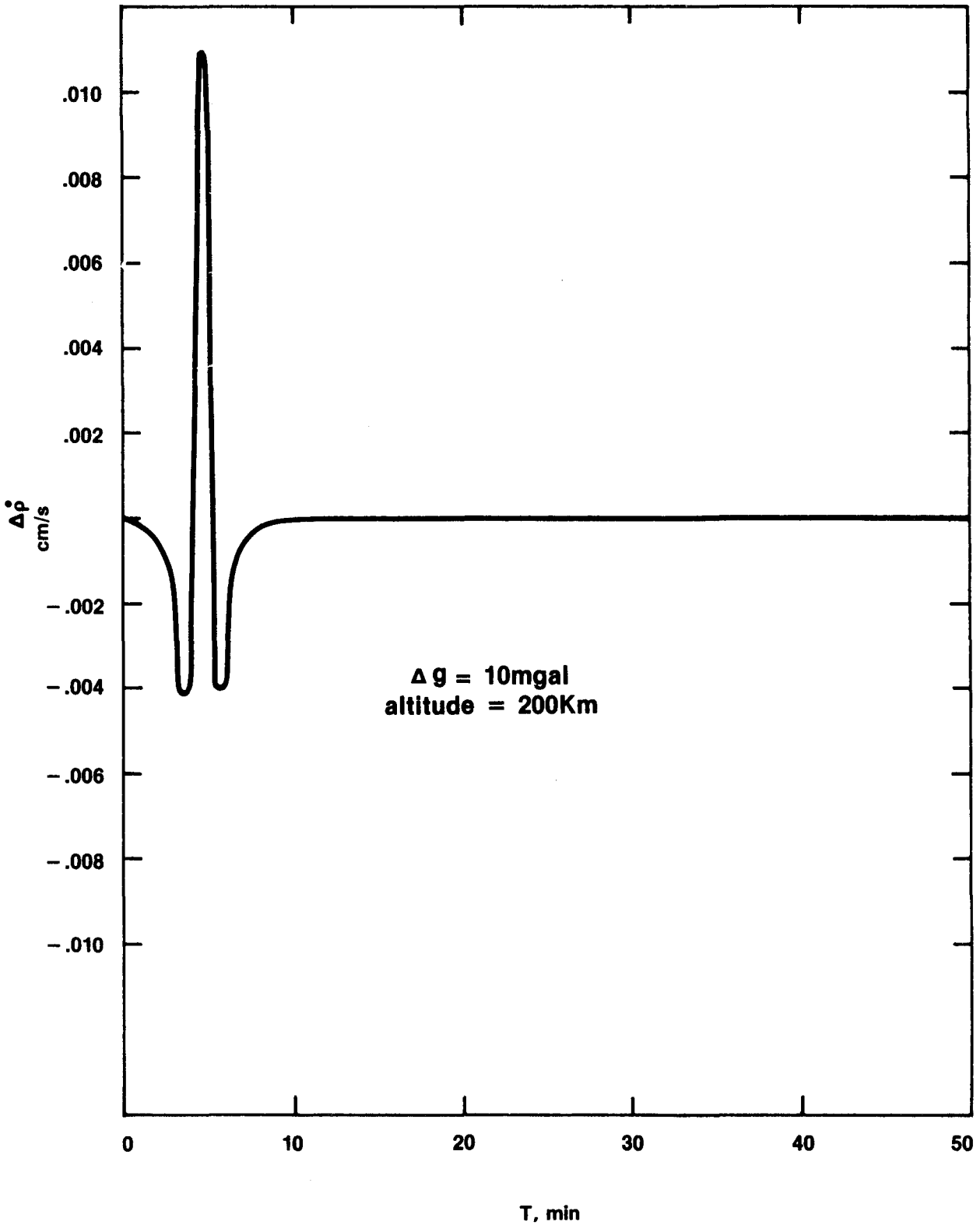

Figure 5.--Intersatellite range-rate differences taken every minute for satellites spaced 3° apart.

range-rate differences, the ratio of the 10-mgal, 1°x1° block signal to a station coordinate error signal is about 400. The conclusion reached from this discussion is that we do not need to consider further the effect of error in tracking station coordinates on our simulation of the recovery of gravity anomalies. Such errors, including tracking-data systematic errors that also produce long wavelength ephemeris errors, are readily filtered from the basic data type, the intersatellite range-rate. Our simulations, therefore, consider only the contribution of the statistical uncertainty of the intersatellite range-rate data to the uncertainty of the estimated 1°x1° mean gravity anomalies. We filtered the signal by taking successive differences. Incidentally, this simple filter was merely a convenience. Much better filters can be constructed.

SIMULATION RESULTS

We have seen that the perturbation of the intersatellite velocity depends on the relative separation of the satellites. Figure 3 shows that the perturbation is maximized for 1°x1° blocks and 200-km altitude by a separation exceeding 5°. However, the accuracy of the intersatellite tracking device itself depends on the separation of the satellites. We assumed intersatellite tracking of 10^{-3} mm/s precision with an integration time (i.e., data interval) of 8 seconds. According to estimates made at The Johns Hopkins University/Applied Physics Laboratory, this rate and precision are obtainable with a microwave device for a separation of 3° or less (Fischell 1979). Figure 3 shows that this separation does not give the maximum amplitude intersatellite range-rate signal. The maximum possible range-rate signal is about 50 percent greater.

The region chosen for our initial simulation experiments was 15°x15°, containing 225 unknown mean anomalies, and centered at 0° latitude and longitude. Figure 6 shows the upper right side (NE quadrant) of this region and the geometry of the downward satellite tracks. Six downward tracks were selected over each 1° for the central 4° of longitude and three tracks over each subsequent degree giving a total of 64 downward tracks over the region. Figure 6 shows that the Earth's rotation has the effect of causing the

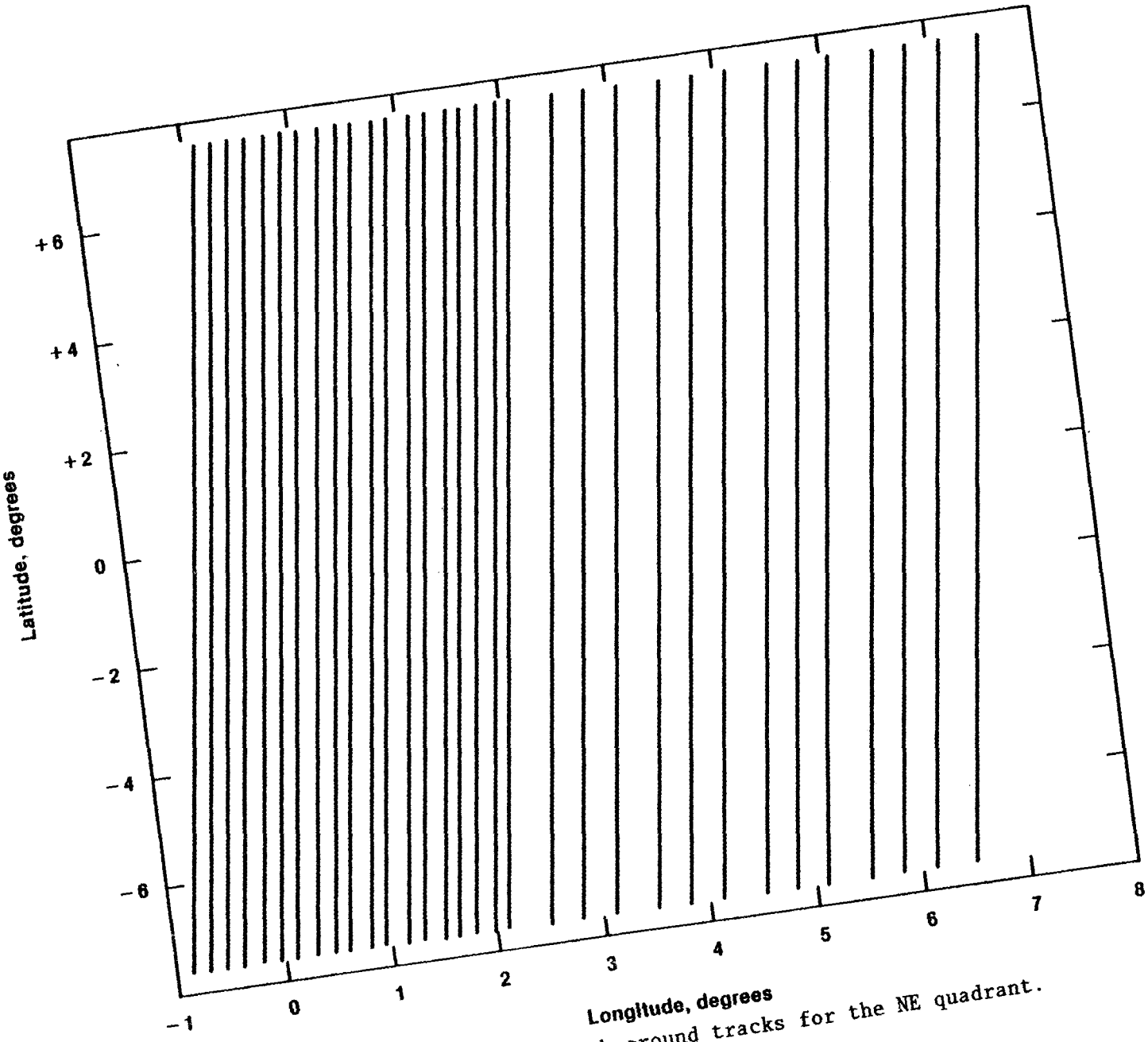

Figure 6.--North-to-south ground tracks for the NE quadrant.

ground tracks of the polar orbiting satellite to be slightly inclined to a meridian. Note that the right edge of the region is carried away from the tracks, resulting in poor sampling. This is one of the reasons our results are valid only for the central area of the 15°x15° region.

Our first simulation (fig. 7) shows the results for the case of 64 arcs of the two polar orbiting satellites at 200-km altitude, spaced 3° apart, and passing in the north-south direction over the region. The numbers in each square (many are omitted for clarity) are the standard deviations of the mean gravity anomalies in milligals for each block. These were taken from the computed covariance matrix of the solution, assuming an intersatellite range-rate measurement precision of 10^{-3} mm/s, but filtered by taking 1 minute differences every 8 seconds. The results for the central region are about 6 mgal.

Figure 8 shows the standard deviations in milligals for the 1°x1° mean anomalies after adding to the simulation in figure 7 the equivalent 64 north-going passes of the two satellites. This 128-arc simulation is improved by a factor of 2 rather than the 40 percent improvement expected by doubling the amount of data.

The 128-arc simulation gives 12 passes over each of the central 6° of longitude with the remaining passes distributed evenly over the outer blocks. This reduction for the outer blocks was done only for economy and, if anything, makes the results conservative.

The 128-arc simulation is encouraging because the standard deviations for the central region are about 3 mgal. The peripheral-region results are better, but only because the blocks outside the 15°x15° region are not adjusted. Again, the peripheral block σ's are not realistic. In addition, the right-side edge values are larger than the left-side values. As noted previously, this occurs because the rotation of the Earth carries the region away from the satellite passes.

Of equal importance to the σ's are the correlation coefficients. We anticipated high values because the perturbation caused by a 1°x1° block

2.3	5.0	7.1	7.4	7.3	7.1	7.1	7.2	3.6	8.0	8.5	9.3	10.0	10.6	7.9
3.1							6.6							7.8
3.3							5.4							7.0
2.8							5.5							6.3
3.2							5.0							6.6
2.8					5.4	5.4	5.5	5.7	6.0					6.1
3.4					6.3	6.2	6.2	6.5	6.9					7.4
3.8	6.4	6.6	7.2	6.7	6.4	6.4	6.4	6.6	7.0	7.6	8.1	8.4	9.1	7.7
3.4					5.4	5.3	5.3	5.5	5.8					6.3
3.0					6.1	6.1	6.1	6.3	6.7					7.2
2.7							4.6							5.2
2.7							5.1							6.2
2.9							5.5							6.4
2.6							4.8							4.6
1.3	2.5	3.2	3.3	3.2	3.1	3.1	3.1	3.2	3.4	3.6	4.1	4.1	4.0	2.8

Figure 7.--Standard deviations in milligals for 1°x1° mean anomalies with 64 north-to-south satellite tracks.

.7	1.4	1.7	1.8	1.8	1.7	1.7	1.7	1.8	1.9	2.0	2.1	2.0	1.8	1.0
1.3							2.6							2.0
1.6							2.7							2.4
1.4							2.5							2.3
1.5							2.5							2.3
1.4							2.5							2.3
1.5						2.7	2.8	2.8						2.5
1.8	2.7	3.1	3.0	3.0	2.9	3.0	3.0	3.1	3.2	3.6	3.8	3.8	3.6	2.8
1.5						2.7	2.8	2.9						2.5
1.4							2.5							2.3
1.5							2.5							2.3
1.4							2.5							2.3
1.6							2.7							2.4
1.3							2.6							2.0
.7	1.4	1.7	1.7	1.7	1.7	1.7	1.7	1.8	1.9	2.0	2.1	2.0	1.8	1.0

Figure 8.--Standard deviations in milligals for the 128-arc case.

endures for a relatively long scale compared to the block size. Figure 9 shows the correlation coefficients of the center block with the other blocks for the simulation of figure 8. The correlation of the center block with its east or west neighbor is very high (-0.88). Thus, the block estimation errors caused by data noise will have almost the same magnitude of error but in an opposite direction to its immediate neighbor in the east-west direction. We should expect, therefore, that the results for 2°x2°, or larger, blocks would be better. This is confirmed below.

Considering the still significant correlations at the north-south borders in figure 9 compared to the smaller values at the east-west borders, we need to consider now whether or not the overall region of 15°x15° was really large enough for the center blocks to have the statistical properties of a global solution. Figure 10 shows the results for a 64-arc (north-to-south only) simulation of the solution for 375 1°x1° blocks with the orbital arcs and the region extended from 15°x15° to 15°x25°. (This limited case of one direction was chosen for economy.) We can compare this directly with the equivalent 64-arc case of 225 1°x1° blocks shown in figure 6. We see that the 15°x25° case is actually improved by one-third as compared to the 15°x15° situation. Recalling that the 128-arc 15°x15° combined solution, which used both the north-going and south-going passes, was twice as good as either the north- or south-going solution independently, we can reasonably conclude that a complete 128-arc, 15°x25° region solution would be about 2 mgal for the uncertainty of the blocks in the central area. However, the east-west correlations are not significantly improved.

Having obtained a basic result of a few milligals for the 200-km altitude, we now consider the impact for missions at other altitudes. Figure 11 shows the σ's for the 128-arc case (considered previously in fig. 8) with the orbiting pair instead at 150-km altitude. Figure 12 gives the results for an altitude of 250 km. The 150-km case is better by about a factor of 5 and the 250-km case is worse by about a factor of 5 than the 200-km situation. In addition, the correlation with the neighboring block drops to 0.81 for the 150-km example and rises to 0.92 for the 250-km altitude. The sharp improvement obtained by decreasing the altitude toward the scale of the

.02	−.03	.05	−.08	.14	−.23	.31	−37	.34	−.27	.20	−.14	.09	.06	.04
							.61							
							−.63							
							.07							
							.48							
					−.19	.24	−.26	.22	−.18					
					−.41	.55	−.63	.55	−.42					
−.07	.12	−.19	.31	−.46	.67	−.88	1.0	−.88	.67	−.47	.31	−.20	.13	−.08
					−.41	.55	−.62	.55	−.42					
					−.19	.24	−.26	.23	−.18					
							.48							
							.07							
							−.63							
							.61							
.03	−.04	.06	−.10	.15	−.23	.31	−.37	.34	−.27	.20	−.14	.09	−.06	.04

Figure 9.--Correlation coefficients of the center anomaly.
Most values omitted for clarity.

							2.5							
							4.0							
							4.2							
							4.0							
							3.8							
							4.0							
							4.1							
							4.2							
							4.1							
							4.1							
							4.2							
						3.9	4.0	4.6						
2.1	4.1	5.3	5.5	5.2	4.6	4.1	4.3	5.1	6.0	7.1	7.9	8.4	8.5	7.1
						4.1	4.2	4.9						
							4.2							
							4.2							
							4.3							
							4.5							
							4.7							
							4.0							
							3.8							
							4.3							
							4.2							
							4.3							
							2.9							

Figure 10.--Standard deviations obtained for a 15°x25° solution with 64 north-south passes.

							.40							
							.55							
							.54							
							.52							
							.52							
							.52							
						.60	.59	.59						
.50	.70	.77	.73	.66	.63	.62	.62	.63	.67	.75	.82	.84	.82	.73
						.59	.59	.60						
							.52							
							.52							
							.52							
							.55							
							.55							
							.40							

Figure 11.--Standard deviations for a 128-arc case with 150-km altitude.

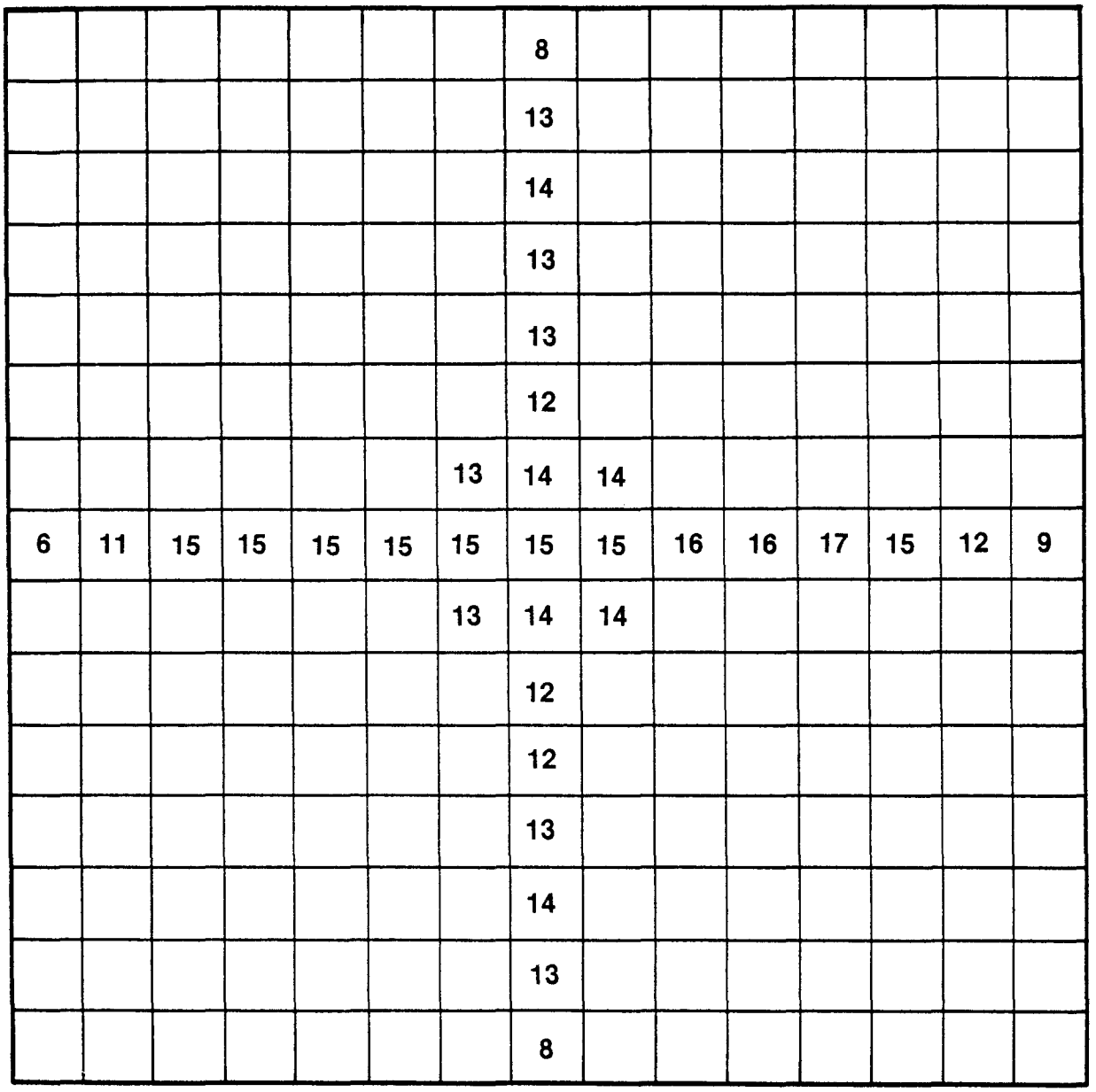

Figure 12.--Standard deviations obtained for a 128-arc solution at 250-km altitude.

1°x1° blocks (~ 111 km/deg at the surface) tends to confirm Schwarz's (1971) rule that the horizontal resolution of the low-low satellite experiment is approximately equal to the altitude of the orbiting pair.

Our final consideration was the possible performance of a so-called "high-low" system where one of the satellites is geosynchronous. Several advantages of this method have been alleged. Indeed, for a given intersatellite speed measurement specification, the high-low case should be superior overall because, for blocks away from the Equator, both the horizontal and vertical components of the intersatellite velocity perturbation are observed. Figure 13 gives the results obtained for a 64-arc case (south-going passes alone) with the geosynchronous member of the pair placed directly over the center of the 15°x15° region and the low satellite at 150-km altitude. Comparison with figure 10 shows that this high-low configuration of 64-arcs is as effective as a 128-arc low-low experiment with all else being equal. But we emphasize these results depend entirely on intersatellite range-rate measurements of 10^{-3} mm/s precision. This precision appears to be obtainable with laser interferometric or sophisticated microwave devices for satellites orbiting close to each other, but probably further technological development is required for observations to a geosynchronous satellite instead of another near-Earth one.

It is interesting to compute the results obtainable when the block size is changed to 2°x2°. If the 1°x1° block errors were uncorrelated, mean 2°x2° anomalies would have a standard deviation of ½ of the 1°x1° anomalies comprising them. However, because of the large negative correlation of adjacent blocks, 2°x2° mean anomalies have a precision of 0.29 mgal, an improvement of 10 compared to the 1°x1° case. Because the 200-km altitude corresponds almost exactly to the dimension of a 2°x2° block, this result provides another demonstration of Schwarz's rule.

DISCUSSION

It would be desirable to be able to give a firm number for the capability of an intersatellite tracking mission to determine the geopotential, but our

							.40							
							.68							
							.53							
							.45							
							.54							
						.72	.71	.74						
						.63	.63	.64						
.56	.73	.76	.74	.62	.59	.58	.58	.59	.59	.73	.79	.82	.87	.84
						.62	.62	.62						
						.75	.74	.75						
							.69							
							.65							
							.68							
							.76							
							.58							

Figure 13.--Standard deviations obtained for the 64-arc high-low case. Altitude of the low satellite was 150 km.

study did not achieve this. However, from a conservative viewpoint we believe that we have answered an important question: Is the capability of satellite-to-satellite tracking for determining the geopotential at the 1°x1°-resolution level near 10 mgal or 1 mgal? Our answer is the latter, especially because our simulations were so conservative. For example, the number of passes over the blocks in our simulation would be attained in a real mission in about 4 months. Much longer missions are within the capability of surface-force compensation systems, so better results could be expected from longer missions. In addition, a somewhat lower altitude could be chosen. Recall that dropping from 200 km to 150 km caused a five-fold improvement. An intermediate altitude choice of about 180 km, rather than 200 km, could result in a substantial improvement, but at the cost of a 50 percent increase in atmospheric drag force. Improvements are also possible in intersatellite measurement capabilities. This would enable an increase in the intersatellite separation and would improve the signal/ noise for the experiment. Finally, a careful inclusion of a priori information taken from the vast store of existing geopotential data would improve the situation. Thus, it seems apparent that a suitably optimized 1 year low-low satellite mission could produce mean anomalies at the 1-mgal level of precision. The high correlations in the east-west direction are unfortunately large, but are tolerable because the σ's are so small compared to the actual variation of gravity anomalies (about 30 mgal rms in 1°x1° blocks).

Some remarks should be made on the significance of a global 1°x1° precise gravity field. Such a field does not necessarily produce an ocean geoid suitable as a reference surface for satellite altimetry at the 1° wavelength. Chovitz (1973) showed that Kaula's (1966) rule-of-thumb $10^{-5}/\ell^2$ for the degree variances of geopotential coefficients implies unaccounted-for geoid undulations of $64/\ell$ meters for a geoid computed to degree ℓ. For a 1°x1° solution, the undulations shorter than 1° could be about 30 cm. At wavelengths longer than 1°, the geoid obtained from 1°x1° mean anomalies would be highly accurate. In addition, the existence of a geopotential field accurate up to the 1°x1° scale would effectively solve the problem of satellite orbit determination. With such a field and a satellite equipped with a

surface-force compensation device, a satellite ephemeris accurate to better than 10 cm could be obtained. Also, the computation of gravimetric geoids such as the one by Marsh and Chang (1978), now widely used as a reference surface for satellite altimetry, could be improved because the effects of mean anomalies in regions distant from a geoid computation point would be accurately known. Finally, a global 1°x1° field would be of interest to geophysicists.

ACKNOWLEDGMENT

This research was partially funded by the National Aeronautics and Space Administration, Washington, D.C., under purchase order no. S59873B. The The authors benefited from conversations with Prof. R. Rapp of Ohio State University.

REFERENCES

Argentiero, P. and Lowrey, B., 1978: A comparison of satellite systems for gravity field measurements, Geophysical Surveys, 3, 207-223.

Belousov, S. L., 1962: Tables of Normalized Associated Legendre Polynomials. The Macmillan Company, New York, (translated from Russian by D. E. Brown), 1-14.

Chovitz, B., 1973: Downward continuation of the potential from satellite altitudes, Boll. Geod. Sci. Affini, 32, 81-88.

Chovitz, B., Lucas, J., and Morrison, F., 1973: Gravity gradients at satellite altitudes. NOAA Technical Report NOS 59, National Ocean Survey, National Oceanic and Atmospheric Administration, Rockville, Md., 24 pp.

Fischell, R. (The John Hopkins University/Applied Physics Laboratory, Silver Spring, Md.), 1979 (personal communication).

Giacaglia, G. E. O. and Lundquist, C. A., 1972: Sampling Functions for Geophysics. Smithsonian Astrophysical Observatory Special Report 344, Cambridge, Mass.

Hotine, M. and Morrison, F., 1969: First integrals of the equations of satellite motion, Bulletin Géodésique,No. 91, 41-45.

Kaula, W. M., 1963: The investigation of the gravitational fields of the moon and planets with artificial satellites, Advan. Space Sci. Technol., 5, 210-226.

Kaula, W. M., Cherubim, G., Burkhand, N., and Jackson, D. D., 1978: Application of inverse theory to new satellite systems for determination of the gravity field. Report No. AFGL-TR-78-0073, U.S. Air Force, Hanscomb Air Force Base, MA 01731.

Koch, K. R. and Witte, B., 1971: Earth's gravity field represented by a simple layer potential from Doppler tracking of satellites, J. Geophys. Res., 76, 8471-8479.

Marsh, J. G. and Chang, E. S., 1976: Detailed gravimetric geoid confirmation of sea surface topography detected by the Skylab S-193 altimeter in the Atlantic Ocean, Bulletin Géodésique, No. 50, 291-299.

Moritz, H., 1978: Least-squares collocation, Reviews of Geophysics and Space Physics, 16, 421-430.

Morrison, F. (National Geodetic Survey, NOS/NOAA, Rockville, Md.) 1979 (paper in preparation).

Morrison, F., 1977: Algorithms for computing the geopotential using a simple-layer density model. NOAA Technical Report NOS 67 NGS 3. National Ocean Survey, National Oceanic and Atmospheric Administration, Rockville, Md., 41 pp.

Morrison, F., 1976: Algorithms for computing the geopotential using a simple layer density model, J. Geophys. Res., 81, 4933-4936.

Orlin, H., 1959: The three components of the external anomalous gravity field, J. Geophys. Res., 64, 2393-2399.

Rapp, R. H., 1979: GEOS 3 data processing for the recovery of geoid undulations and gravity anomalies, J. Geophys. Res., 84, 3784-3792.

Schwarz, C. R., 1972: Refinement of the gravity field by satellite-to-satellite Doppler tracking, Geophysical Monograph, 15, American Geophysical Union, Washington, D.C.

Wolff, M. ,1969: Direct measurements of the Earth's gravitational potential using a satellite pair, J. Geophys. Res., 74, 5295-5300.

(Continued from inside front cover)

NOS NGS-3 Adjustment of geodetic field data using a sequential method. Marvin C. Whiting and Allen J. Pope, March 1976, 11 pp (PB253967). A sequential adjustment is adopted for use by NGS field parties.

NOS NGS-4 Reducing the profile of sparse symmetric matrices. Richard A. Snay, June 1976, 24 pp (PB-258476). An algorithm for improving the profile of a sparse symmetric matrix is introduced and tested against the widely used reverse Cuthill-McKee algorithm.

NOS NGS-5 National Geodetic Survey data: availability, explanation, and application. Joseph F. Dracup, June 1976, 45 pp (PB258475). The summary gives data and services available from from NGS, accuracy of surveys, and uses of specific data.

NOS NGS-6 Determination of North American Datum 1983 coordinates of map corners. T. Vincenty, October 1976, 8 pp (PB262442). Predictions of changes in coordinates of map corners are detailed.

NOS NGS-7 Recent elevation change in Southern California. S.R. Holdahl, February 1977, 19 pp (PB265-940). Velocities of elevation change were determined from Southern Calif. leveling data for 1906-62 and 1959-76 epochs.

NOS NGS-8 Establishment of calibration base lines. Joseph F. Dracup, Charles J. Fronczek, and Raymond W. Tomlinson, August 1977, 22 pp (PB277130). Specifications are given for establishing calibration base lines.

NOS NGS-9 National Geodetic Survey publications on surveying and geodesy 1976. September 1977, 17 pp (PB275181). Compilation lists publications authored by NGS staff in 1976, source availability for out-of-print Coast and Geodetic Survey publications, and subscription information on the Geodetic Control Data Automatic Mailing List.

NOS NGS-10 Use of calibration base lines. Charles J. Fronczek, December 1977, 38 pp (PB279574). Detailed explanation allows the user to evaluate electromagnetic distance measuring instruments.

NOS NGS-11 Applicability of array algebra. Richard A. Snay, February 1978, 22 pp (PB281196). Conditions required for the transformation from matrix equations into computationally more efficient array equations are considered.

NOS NGS-12 The TRAV-10 horizontal network adjustment program. Charles R. Schwarz, April 1978, 52 pp (PB283087). The design, objectives, and specifications of the horizontal control adjustment program are presented.

NOS NGS-13 Application of three-dimensional geodesy to adjustments of horizontal networks. T. Vincenty and B. R. Bowring, June 1978, 7 pp (PB286672). A method is given for adjusting measurements in three-dimensional space without reducing them to any computational surface.

NOS NGS-14 Solvability analysis of geodetic networks using logical geometry. Richard A. Snay, October 1978, 29 pp (PB291286). No algorithm based solely on logical geometry has been found that can unerringly distinguish between solvable and unsolvable horizontal networks. For leveling networks such an algorithm is well known.

NOS NGS-15 Goldstone validation survey - phase 1. William E. Carter and James E. Pettey, November 1978, 44 pp (PB292310). Results are given for a space system validation study conducted at the Goldstone, Calif., Deep Space Communication Complex.

NOS NGS-16 Determination of North American Datum 1983 coordinates of map corners (Second Prediction). T. Vincenty, April 1979, 6 pp (PB297245). New predictions of changes in coordinates of of map corners are given.

NOS NGS-17 The HAVAGO three-dimensional adjustment program. T. Vincenty, May 1979, 18 pp (PB297069). The HAVAGO computer program adjusts numerous kinds of geodetic observations for high precision special surveys and ordinary surveys.

NOS NGS-18 Determination of astronomic positions for California-Nevada boundary monuments near Lake Tahoe. James E. Pettey, March, 1979, 22 pp (PB301264). Astronomic observations of the 120th meridian were made at the request of the Calif. State Lands Commission.

NOS NGS-19 HOACOS: A program for adjusting horizontal networks in three dimensions. T. Vincenty, July 1979, 18 pp (PB301351). Horizontal networks are adjusted simply and efficiently in the height-controlled spatial system without reducing observations to the ellipsoid.

NOS NGS-20 Geodetic leveling and the sea level slope along the California coast. Emery I. Balazs and Bruce C. Douglas, September 1979, 23 pp. Heights of four local mean sea levels for the 1941-59 epoch in California are determined and compared from five geodetic level lines observed (leveled) between 1968-78.

NOS NGS-21 Haystack-Westford Survey. W. E. Carter, C. J. Fronczek, and J. E. Pettey, September 1979, 57 pp. A special purpose survey was conducted for VLBI test comparison.

NOS NGS-22 Gravimetric tidal loading computed from integrated Green's functions. C. C. Goad, October 1979, 15 pp. Tidal loading is computed using integrated Green's functions.

NOS NGS-23 Use of auxiliary ellipsoids in height-controlled spatial adjustments. B. R. Bowring and T. Vincenty, November 1979, 6 pp. Auxiliary ellipsoids are used in adjustments of networks in the height-controlled three-dimensional system for controlling heights and simplifying transformation of coordinates.

(Continued on inside back cover)

*U.S. GOVERNMENT PRINTING OFFICE: 1980 311-046/364 1-3

(Continued)

NOAA Technical Reports, NOS/NGS subseries

NOS 65 NGS 1 The statistics of residuals and the detection of outliers. Allen J. Pope, May 1976, 133 pp (PB258428). A criterion for rejection of bad geodetic data is derived on the basis of residuals from a simultaneous least-squares adjustment. Subroutine TAURE is included.

NOS 66 NGS 2 Effect of Geoceiver observations upon the classical triangulation network. R. E. Moose and S. W. Henriksen, June 1976, 65 pp (PB260921). The use of Geoceiver observations is investigated as a means of improving triangulation network adjustment results.

NOS 67 NGS 3 Algorithms for computing the geopotential using a simple-layer density model. Foster Morrison, March 1977, 41 pp (PB266967). Several algorithms are developed for computing with high accuracy the gravitational attraction of a simple-density layer at arbitrary altitudes. Computer program is included.

NOS 68 NGS 4 Test results of first-order class III leveling. Charles T. Whalen and Emery Balazs, November 1976, 30 pp (GPO# 003-017-00393-1) (PB265421). Specifications for releveling the National vertical control net were tested and the results published.

NOS 70 NGS 5 Selenocentric geodetic reference system. Frederick J. Doyle, Atef A. Elassal, and James R. Lucas, February 1977, 53 pp (PB266046). Reference system was established by simultaneous adjustment of 1,233 metric-camera photographs of the lunar surface from which 2,662 terrain points were positioned.

NOS 71 NGS 6 Application of digital filtering to satellite geodesy. C. C. Goad, May 1977, 73 pp (PB-270192). Variations in the orbit of GEOS-3 were analyzed for M_2 tidal harmonic coefficient values which perturb the orbits of artificial satellites and the Moon.

NOS 72 NGS 7 Systems for the determination of polar motion. Soren W. Henriksen, May 1977, 55 pp (PB274698). Methods for determining polar motion are described and their advantages and disadvantages compared.

NOS 73 NGS 8 Control leveling. Charles T. Whalen, May 1978, 23 pp (GPO# 003-017-00422-8) (PB286838). The history of the National network of geodetic control, from its origin in 1878, is presented in addition to the latest observational and computational procedures.

NOS 74 NGS 9 Survey of the McDonald Observatory radial line scheme by relative lateration techniques. William E. Carter and T. Vincenty, June 1978, 33 pp (PB287427). Results of experimental application of the "ratio method" of electromagnetic distance measurements are given for high resolution crustal deformation studies in the vicinity of the McDonald Lunar Laser Ranging and Harvard Radio Astronomy Stations.

NOS 75 NGS 10 An algorithm to compute the eigenvectors of a symmetric matrix. E. Schmid, August 1978, 5 pp (PB287923). Method describes computations for eigenvalues and eigenvectors of a symmetric matrix.

NOS 76 NGS 11 The application of multiquadric equations and point mass anomaly models to crustal movement studies. Rolland L. Hardy, November 1978, 63 pp (PB293544). Multiquadric equations, both harmonic and nonharmonic, are suitable as geometric prediction functions for surface deformation and have potentiality for usage in analysis of subsurface mass redistribution associated with crustal movements.

NOS 79 NGS 12 Optimization of horizontal control networks by nonlinear programing. Dennis G. Milbert, August 1979, 44 pp. Several horizontal geodetic control networks are optimized at minimum cost while maintaining desired accuracy standards.

NOAA Manuals, NOS/NGS subseries

NOS NGS 1 Geodetic bench marks. Lt. Richard P. Floyd, September 1978, 56 pp (GPO# 003-017-00442-2) (PB296427). Reference guide provides specifications for highly stable bench marks, including chapters on installation procedures, vertical instability, and site selection considerations.

U.S. DEPARTMENT OF COMMERCE
National Oceanic and Atmospheric Administration
National Ocean Survey
National Geodetic Survey, C13x4
Rockville, Maryland 20852

OFFICIAL BUSINESS